# Fluctuations and scaling in creep deformation

Jari Rosti,[1,*] Juha Koivisto,[1,†] Lasse Laurson,[2,‡] and Mikko J. Alava[1,§]

[1]*Department of Applied Physics, Aalto University, PO Box 14100, Aalto 00076, Finland*
[2]*ISI Foundation, Viale S. Severo 65, 10133 Torino, Italy*

(Dated: July 28, 2010)

The spatial fluctuations of deformation are studied in creep in the Andrade's power-law and the logarithmic phases, using paper samples. Measurements by the Digital Image Correlation technique show that the relative strength of the strain rate fluctuations increases with time, in both creep regimes. In the Andrade creep phase characterized by a power law decay of the strain rate $\epsilon_t \sim t^{-\theta}$, with $\theta \approx 0.7$, the fluctuations obey $\Delta\epsilon_t \sim t^{-\gamma}$, with $\gamma \approx 0.5$. The local deformation follows a data collapse appropriate for an absorbing state/depinning transition. Similar behavior is found in a crystal plasticity model, with a jamming or yielding phase transition.

PACS numbers: 62.20.Hg,68.35.Rh,05.70.Ln,05.40.-a

The creep of a sample under a constant load exhibits often three rheological phases in materials from metals and alloys with a crystalline structure to rocks and composites: the initial power-law decrease of the strain rate or primary creep, quasi-stationary secondary creep, and finally tertiary creep approaching final failure. It is important to understand such empirical laws of scaling in material deformation. The Andrade creep law, stating that the deformation rate decays in time as $\frac{d\epsilon(t)}{dt} \equiv \epsilon_t \sim t^{-\theta}$, with $\theta \approx 2/3$, originates already from 1910 [1]. The phenomenological creep laws [2] are valid for many materials from metals to polymeric materials to composites like ordinary paper [3] to rocks [4]. In the case of metals the dynamics is related to dislocations and the structures they form. It is intriguing why there should be such universality, which seems to be "coarse-grained", not dependent on the microscopic details.

In this vein, collective phenomena as fluctuations and avalanches [5] have been recently studied in crystal plasticity [6–10], viscoelastic fluids and networks [11–13], granular materials and amorphous glasses [14] and in fracture [15–18]. The dynamics of simple dislocation assemblies exhibits a phase transition at a critical external shear stress value $\sigma_c$, similar to the jamming one seen in granular media and glasses [19–21], with the order parameter (the deformation rate) exhibiting a power-law decay in time close to the transition, as the Andrade law [22, 23].

To explore the physics of creep and to see if it could be related to such collective behavior, we measure local creep rates in primary creep. The main question is: what kind of fluctuations does the creep show, and how do they scale with time? In non-crystalline materials strain variations implies a localization of deformation which is unrelated to dislocation activity. So, another issue is: what kind of universality exists in creep deformation and in local creep strain rates? By digital image correlation analysis, we show that the spatial fluctuations of creep strain rates follow a scaling law during the Andrade creep. The ratio of fluctuations to mean rate increases with time. This feature persists in the logarithmic creep regime, where $\epsilon(t) \sim \log(t)$, or $\epsilon_t \sim t^{-1}$. The critical properties of the power-law creep are tested by applying the theory of non-equilibrium phase transitions. We find that spatial creep deformation statistics follows its own scaling and a scaling function. Similar behavior is encountered in a simple discrete dislocation or crystal plasticity model, which exhibits Andrade creep for applied stress values close to the critical stress $\sigma_c$ of the dislocation jamming transition. This stress separates an active phase with a constant average creep rate from a low-stress phase where the deformation rate dies out after a transient [22]. The temperature enters indirectly only via the dislocation mobility. The most natural explanation is that Andrade creep derives from a non-equilibrium phase transition between "jammed", or frozen, and "flowing", or active, states [19]. Usual materials science constitutive equations and creep laws are based on phenomenological equations, usually related to an thermally activated process [24]. They may fail to cope with correlated, intermittent, dynamics.

To induce creep in experiments, we applied a constant stress to a sheet of paper in a tensile-test geometry (Fig. 1a). Tests were made in humidity and temperature controlled conditions, $33 \pm 1$ % of relative humidity and $33 \pm 1$ $^o$C of temperature, with the typical applied loads around 40 N, corresponding to a stress of 13 MPa. We used ordinary office paper, with $30 \times 100$ mm$^2$ samples loaded in the cross-machine direction. The sample is imaged with SensiCam 370KL0562 digital camera with a low thermal noise ratio, at 12 bit gray scale resolution. The exposure time in measurements was 200 ms, and the sampling frequency of the digital imaging was $0.1$ Hz.

In sample scale images, a printed speckle pattern (Fig. 1b) was used due to its sharp contrast and translational invariance. A set of experiments with larger magnification and smaller load was also made with an image size of 3x4 mm and using specially prepared sheets, with 5 % of the fibres colored for contrast. The larger magnification and a smaller load make it possible to follow the entire experiment with Digital Image Correlation (DIC), beyond the primary creep regime.

Experimentally, a time-series of displacement fields is derived using the DIC-technique [25–27] (Fig. 1a). The algorithm describes both the image and the deformation using the B-spline model. The algorithm finds the deformation function by using the multiresolution approach for the minimization, so that the image and the deformation model is refined every time the convergence is reached. The criteria for the convergence

is the sum of squared differences (SSD), i.e. the deformation function is applied to the original image and the SSD is computed against the deformed image. The algorithm is described in Ref. [28]. A discrete picture, in space and time, ensues of the local creep strain rates [29]. An example (Fig. 1b) shows the variations of the rates for one $\Delta t$. For the spatial fluctuations of the local strain rate $\epsilon_t^{i,j}$, we define an evenly spaced grid on an image, which consists of $49\times78$ points. The standard deviation of local strain rates $\Delta\epsilon_t$ is computed over the grid values on the lower half on the sample where absolute displacements are large. This is further illustrated in Figure 1a, which shows how the creep fluctuations are measured from the experiment.

A feature visible in experiments is the disordered structure of paper, two-dimensional over scales larger than the out-of-plane thickness [30]. One should note that the non-uniformity results in a locally varying stress field, even in the elastic deformation regime, in analogy to the internal stresses of materials with dislocations.

The Andrade creep results are confronted with those of the simulations of a two-dimensional discrete dislocation dynamics (DDD) model [6, 22, 31]. The $N$ point-like dislocations with Burgers vectors $\mathbf{b}_n = s_n b\mathbf{u}_x$ (with $s_n = \pm1$ and $n = 1\ldots N$) parallel to the glide direction can be thought to represent a cross-section of a single crystal with straight parallel edge dislocations and a single slip geometry [6]. The dislocations interact through their anisotropic long-range shear stress fields, and perform over-damped glide motion only driven by an applied external shear stress $\sigma$ [6, 23, 29]. Fluctuations are studied in the vein illustrated by Figure 1a by measuring the local strain rates

$$\epsilon_t^{i,j}(t) = \frac{b}{l^2}\sum_{\mathbf{r}_n\in \text{ box } i,j} s_n b\left[\frac{x_n(t+0.5\Delta t) - x_n(t-0.5\Delta t)}{\Delta t}\right] \tag{1}$$

over a time scale $\Delta t$ within sub-volumes of linear size $l$, with $x_n(t)$ the position of the $n$th dislocation within its glide plane.

Figure 2 depicts the Andrade creep results for the standard deviation of the creep rate probability distributions. For both paper samples and DDD simulations (performed at $\sigma = \sigma_c \approx 0.025$, in dimensionless units [29]) we observe a typical Andrade law of the form $\epsilon_t \propto t^{-0.7}$ or an Andrade-exponent $\theta$ close to 2/3. The standard deviation follows also a power-law, and scales as

$$\Delta\epsilon_t \propto t^{-0.5}, \tag{2}$$

so an exponent $\gamma \sim 0.5$ is found. The "second" Andrade or fluctuation exponent $\gamma$ is slightly higher for experiments (0.55), while in the DDD simulations a value of 0.5 is indicated. Evidently this exponent is smaller than that of the mean creep rate. Thus fluctuations increase in relative terms, and creep becomes more intermittent with time. The accuracy of the DIC method poses a limit to following the power-law of Eq. (1), apart from the maximum length of the power-law creep regime obtainable by tuning the parameters. In the DDD model the scaling range is controlled by the proximity of the jamming transition.

At lower stresses, logarithmic creep is found with no signature of the Andrade phase. Figure 3a shows that a fluctuation scaling can be extracted in this regime. Still, the fluctuation magnitude decays slower than the creep rate. Their ratio might be related in each sample to the transition to tertiary creep, which might indicate a zone-like localization of subsequent deformation. The simultaneous measurement of Acoustic Emission indicates no substantial damage accumulation or micro-cracking until close to the transition to tertiary creep. Thus DIC measures the statistics of viscoplastic deformation, and not deformations related to eventual brittle fracture. Microscopically in paper, the fibers and the network structure can both deform irreversibly. For the sample-to-sample variations, we find here a Monkman-Grant relation [15, 32] between the time at which a minimum creep rate occurs in a sample $t_m$ and the final failure time $t_c$, $t_m \propto 0.83\, t_c$. The relevance of fluctuations for the Monkman-Grant law would be interesting to understand.

The theoretical interpretation of the scaling of the creep fluctuations can be analyzed within and with the aid of the DDD model. One question is how this "second Andrade-scaling" is related to the usual primary creep exponent? Assuming intermittent, localized creep activity the active fraction of the regions of the specimen account for the creep strain measured in a time step. This argument leads to a self-consistency condition between the "number" of such active regions as a function of time, and the typical time-dependent creep strain rate in each such region [29]. If the statistics would originate from the decay of the fraction of localized, active regions, themselves deforming at a rate independent of time, it would indicate a $\gamma = 1/3$, half of the Andrade $\theta$, instead of the measured $0.5\ldots0.55$. This line of reasoning is related to classical, dislocation-based theory arguments of Andrade creep [33, 34].

The nature of the creep dynamics seems to exhibit universality typical of phenomena arising from phase transitions. If a wide variety of materials follows such behavior, it calls for a continuum description, independent of microscopic details. Statistical physics offers concepts such as depinning transitions of elastic manifolds in random media. These have been applied to coarse-grained dislocation plasticity [35], and are examples of absorbing-state phase transitions. Similarly to what is seen in the DDD model, such theories present or predict a power-law relaxation of the order parameter close to the critical point. The jamming/absorbing state transition scenario can be further tested by the ansatz that the creep rate is the "order parameter" of the phase transition. One collapses the total deformation histograms, $P(\epsilon, t)$ (scaling out the average deformation at time $t$) as one should do [36] for the integrated order parameter. Both the DIC (Figure 3b) and DDD data ([29]) exhibit a reasonable data collapse, indicating critical behaviour, close to such a phase transition. Further evidence for the origin of the fluctuations in collective phenomena can be sought in the correlation functions $C(x-x', t-t')$

of strain fields, calculated as for an "interface field" $\epsilon(x,t)$. Preliminary results imply, that the temporal scaling yields the Andrade exponent [29]. The fact that the jamming transition picture works for the experiments seems as such surprising for a non-crystalline material, though a possible universality of the Andrade creep would argue for the opposite.

It remains to extend the measurements to study the small scale spatiotemporal features, such as localized events [37]. The creep fluctuations could be investigated in other systems such as two- and three-dimensional colloidal crystals or glasses [38, 39]. Future research directions include considering the fluctuations for various load histories, an example being fatigue, and the role of "aging" and sample-relaxation.

Local creep rates exhibit a fluctuation scaling, both in a disordered, viscoplastic material and in a model of dislocation plasticity. This presents a challenge: what kind of coarse-grained theory for the deformation field would reproduce those signatures? Such fluctuations are beyond classical, phenomenological creep models. The phase transition scenario of Andrade creep relegates the temperature to a secondary role, in the DDD model via the viscous dynamics of the dislocations. In depinning, for stresses below the critical one, thermal fluctuations induce a transient towards a thermally activated steady-state creep [40], which could relate to the logarithmic behavior in experiments.

Non-equilibrium scenarios include various models for the plasticity of amorphous materials [13, 14, 41, 42] where the presence of localized events has been recognized e.g. in the so-called Shear Transformation Zone theory. To summarize, the main issue is that creep deformation exhibits spatial fluctuations which scale in time, indicating that the different phenomenological creep regimes could be understood in terms of phase transitions.

We acknowledge the support of the Academy of Finland via the Center of Excellence program and a post-doctoral grant, and the European Commission NEST Pathfinder programme TRIGS under contract NEST-2005-PATH-COM-043386.

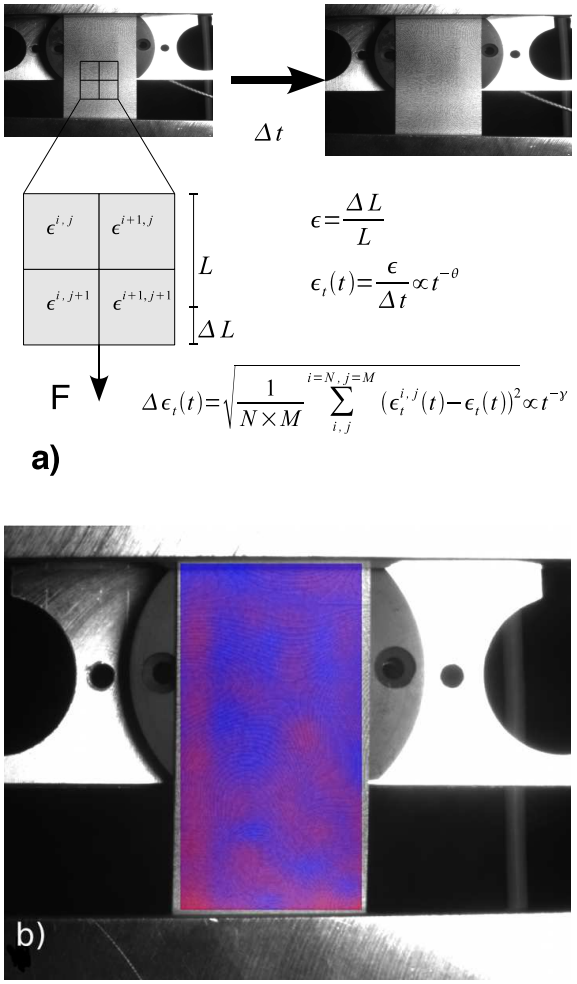


FIG. 1. The experimental scenario. From a pair of digital images at a time-interval $\Delta t$ the local deformations are extracted at a grid of $N \times M$ points, with $N = 49$ and $M = 39$ on the lower half plane of the sample. The strain fluctuations are measured via the time-dependent standard deviation, and compared to the mean creep rate, here in primary/Andrade creep. In the DDD simulations, the system is similarly divided into boxes of linear size $l$, with local strain rates $\epsilon_t^{i,j}$. b) A digital image of a paper sample on a scale of 40 mm$^2$. Superposed is a typical deformation grid for a time difference $\Delta t$ of 10 seconds. The color scale indicates the degree of local creep deformation (blue: small, red: large). In the background: the experimental setup. The visible speckle pattern is printed and designed to have a structure and contrast appropriate for the DIC method.

* jro@fyslab.hut.fi
† jko@fyslab.hut.fi
‡ lasse.laurson@gmail.com
§ mikko.alava@tkk.fi

[1] E. N. da C. Andrade, Proc. R. Soc. **A 84**, 1 (1910).
[2] F. Louchet and P. Duval, Int. J. Mat. Res. **100**, 1433 (2009).
[3] D. W. Coffin, Advances in Paper Sci. and Tech., I'Anson, S.J. (ed.), FRC, Lancashire, UK, p. 651 (2005).
[4] F.R.N. Nabarro and F.De. Villiers, Physics of Creep and Creep-Resistant Alloys. (CRC, 1995).
[5] J.P. Sethna, K.A. Dahmen and C.R. Myers, Nature **410**, 242 (2001).
[6] M. C. Miguel et al., Nature **410**, 667 (2001).
[7] J. Weiss and D. Marsan, Science **299**, 89 (2003).
[8] B. Jakobsen et al., Science **312**, 889 (2006).
[9] D.M. Dimiduk, C. Woodward, R. LeSar and M.D. Uchic, Science **312**, 1188 (2006).
[10] F. Csikor et al., Science **318**, 251 (2007).
[11] P. Coussot, Q.D. Nguyen, H.T. Huynh and D. Bonn, Phys. Rev. Lett. **88**, 175501 (2002).
[12] J. Liu et al., Phys. Rev. Lett. **98**, 198304 (2007).
[13] L. Bocquet, A. Colin, and A. Ajdari, Phys. Rev. Lett. **103**, 036001 (2009).
[14] C. Maloney and A. Lemaitre, Phys. Rev. Lett. **93**, 016001 (2004).
[15] H. Nechad, A. Helmstetter, R. El Guerjouma and D. Sornette, Phys. Rev. Lett. **94**, 045501 (2005).
[16] M.J. Alava, P.K.N.N. Nukala and S. Zapperi, Advances in Physics **55**, 349 (2006).

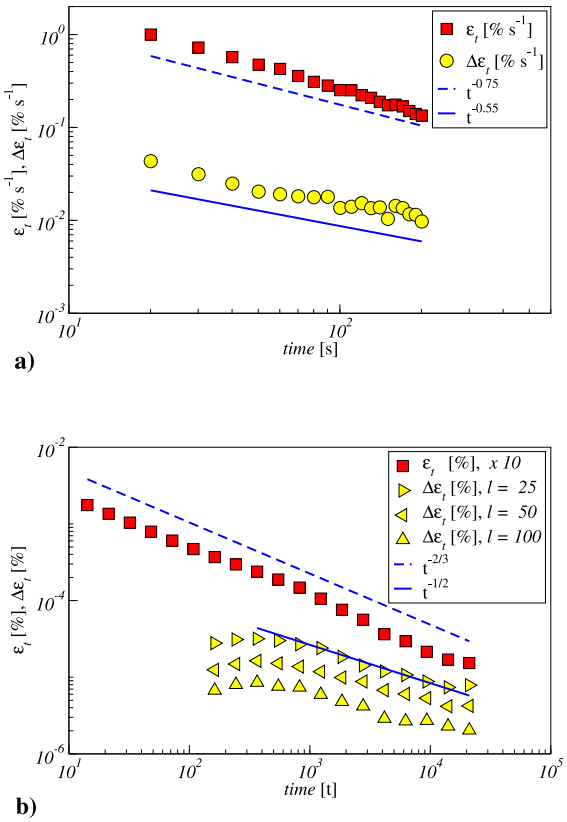


FIG. 2. (Color online) Average creep rate and the standard deviation of the local creep rates. a) Typical experimental data. The sample average lifetime is 800-1600 seconds. The primary-to-secondary creep transition takes place continuously at 150-200 seconds. 16 experiments are used. The effective Andrade exponent is about 0.7 in the range 10 to 50 seconds, and becomes close to one (signalling secondary creep) above 150 seconds. b) The Andrade's law and the fluctuation scaling for the DDD model for three different box sizes to compute the local rates, at $\sigma \approx \sigma_c$. The early-time cross-over in the fluctuations is due to computation time-interval of $\Delta t = 100$.

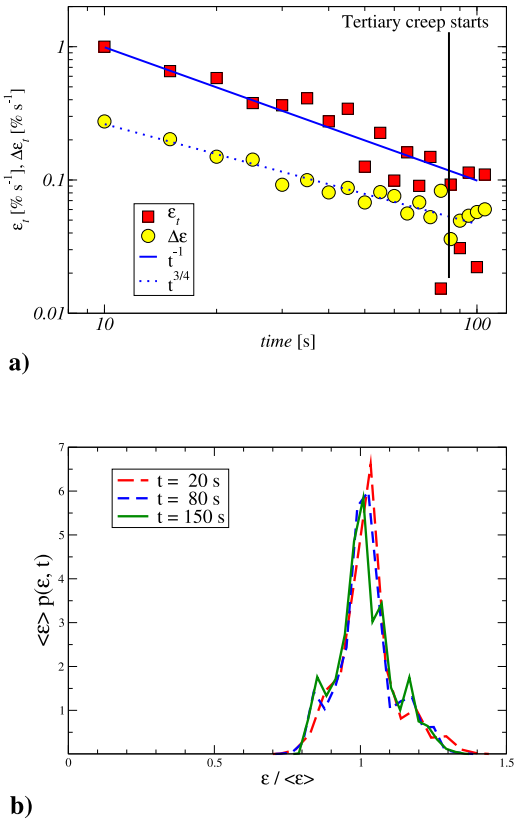


FIG. 3. (Color online) a) Experimental results from logarithmic creep using a smaller imaging area, 5 second image intervals, and a smaller load, showing the average creep rate and the fluctuations. The former decays faster, and at the end these two become comparable, on the observation scale. The data is an average over 9 experiments. b) Data collapse of the primary creep strain distribution $P(\epsilon, t)$ from the experiments. The local deformation distributions can be collapsed using the creep strain as the scaling parameter.


[17] F. Kun et al. J. Stat. Mech.: Theo. Exp. P02003 (2007).
[18] D. Bonamy, S. Santucci and L. Ponson, Phys. Rev. Lett. **101**, 045501 (2008).
[19] A.J. Liu and S. R. Nagel, Nature **396**, 21 (1998).
[20] J. Goyon et al., Nature **454**, 84 (2008).
[21] A.S. Keys et al. Nature Phys. **3**, 260 (2007).
[22] M.-C. Miguel, A. Vespignani, M. Zaiser and S. Zapperi, Phys. Rev. Lett. **89**, 165501 (2002).
[23] L. Laurson, M.C. Miguel and M.J. Alava, Phys. Rev. Lett. **105**, 015501 (2010).
[24] Y.H. Lin, Polymer Viscoelasticity: Basics, Molecular Theories and Experiments. (World Scientific, Singapore, 2003).
[25] M.A. Sutton, J.L. Turner, H.A. Bruck and T.A. Chae, Exp. Mech. **31**, 168 (1991).
[26] J. Kybic and M. Unser, IEEE Trans. Image Process. **12**, 1427 (2003).
[27] F. Hild and S. Roux, Strain **42**, 69 (2006).
[28] J. Kybic, P. Thevenaz, A. Nirkko and M. Unser, IEEE Trans. Med. Imag. **19**, 80 (2000).
[29] J. Rosti et al., in preparation.
[30] M.J. Alava and K.J. Niskanen, Rep. Prog. Phys. **69**, 669 (2006).
[31] E. Van der Giessen and A. Needleman, Model. Simul. Mater. Sci. Eng **3**, 689 (1995).
[32] F.C. Monkman and N.J. Grant, Proc. ASTM **56**, 593 (1956).
[33] N.F. Mott, Proc. R. Soc. Lond. A. **220**, 1 (1953).
[34] A.H. Cottrell, Phil. Mag. Lett. **84**, 685 (2004).
[35] M. Zaiser and P. Moretti, J. Stat. Mech.: Theo. Exp. P08004 (2005).
[36] R. Dickman and M.A. Muńoz, Phys. Rev. E **62**, 7632 (2000).
[37] M. Talamali, V. Petäjä, D. Vandembroucq and S. Roux, Phys. Rev. E **7**8, 016109 (2008).
[38] A. Pertsinidis and X.S. Ling, New J. Phys. **7**, 33 (2005).
[39] P. Schall, D. A. Weitz, and F. Spaepen, Science **318**, 1895 (2007).
[40] A.B. Kolton, A. Rosso and T. Giamarchi, Phys. Rev. Lett. **94**, 047002 (2005).
[41] M.L. Falk and J.S. Langer, Phys. Rev. **E 57**, 7192 (1998).
[42] M. Talamali, V. Petäjä, S. Roux and D. Vandembroucq, arXiv:1005.2463